International Journal of Engineering Innovation & Research
Volume 7, Issue 1, ISSN: 2277 – 5668

Stability Study of LQR and Pole-Placement Genetic Algorithm Synthesized Input-Output Feedback Linearization Controllers for a Rotary Inverted Pendulum System

Yi Yang and Haiyan Henry Zhang*
Multidisciplinary Design Laboratory Purdue University.
*Corresponding author email id: *hhzhang@purdue.edu

Date of publication (dd/mm/yyyy): 16/02/2018

Abstract **– The rotary inverted pendulum (RIP) has a fourth order nonlinear dynamics, and its control is typically with two stages, i.e., a swing-up control and a balancing control. For Linear-quadratic regulator (LQR) control, under large disturbances, the RIP stability may be lost. With Input-output feedback linearization (IOFL) control, the linearized portion's stability is governed by the linear control scheme, and the closed loop for the unlinearizable portion of the original dynamics forms the so-called internal dynamics, which not necessarily has the bounded input - bounded output (BIBO) stability. A modified IOFL control is presented with these approaches: for the linearized portion, the gains associated with the angle and angular velocity of the inverted pendulum are selected based on enhancing the stability via pole placement; for the unlinearizable portion, the gains associated with the angle and angular velocity of the rotary arm are determined by minimizing the cost function via genetic algorithm. Therefore, the pole-placement genetic algorithm synthesized IOFL control promises an augmented stability region for the RIP system. The results can be generalized in the applications of various nonlinear systems' control design.**

Keywords **– Input Output Feedback Linearization, Linear Quadratic Regulator, Genetic Algorithm, Internal Dynamics.**

I. INTRODUCTION

For decades, dynamics of the rotary inverted pendulum (RIP) has been extensively utilized as a test bed for dealing with nonlinear control problems. The RIP, also called the Furuta pendulum, was invented at Tokyo Institute of Technology by Katsuhisa Furuta and his colleagues. Furuta et al. [1] proposed the RIP physical model with a rotary arm driven by a DC motor and a pendulum linked to the end of rotating arm.

Even though the RIP system's contracture is simple, it is a good representative to various dynamic systems. For example, a bassinet, or known as a bed cradle is a bed specifically invented for young-age babies. The rocking-chair movement activated by a RIP-like structure ensures that the baby's body in the cradle moves along a curved trajectory. However, the stability of the rocking-chair movement is prone to be lost when the cradle moves to the far side from the central equilibrium position. Improving the stability of RIP system dynamics is essential to the bassinet design. The rocket landing is another well-known application of the RIP system. The motion of a flying rocket is a superposition of the translation of the mass center and the rotation of the rocket about its mass center. Essentially, the RIP system can be viewed as a simplified physical model of the early rockets, even of the current air-to-air missiles with adjustable fins at the rear for the aerodynamic force control. With the intention of designing a robust and stable guidance system for a rocket, a RIP system which fundamentally embodies similar characteristics as a rocket flying system is always taken to be investigated by aero-dynamists at an early stage. A third application of the RIP system lies in the legged locomotion and gait rehabilitation for patients activated by robotic devices. The leg of a patient or a robot can be seen as a double rigid link. Locomotion in humans and robots involves a periodic occurrences of the translational motion about the touchdown point and the rotational motion for the double link. The inverted pendulum and biped stability are analyzed in [2]. The RIP system, as a comprehensive extension to the traditional inverted pendulum system, can be foreseen its potentials in developing more complicated human rehabilitation systems or robot gait models.

The RIP system is a fourth order nonlinear dynamic system. Generally, for the RIP system, there are two control stages, i.e., a swing-up control and a balancing control. At first, the researchers attempted only to design the swing-up control for the RIP system, and the swing-up controller is meant to provide the pendulum enough initial kinetic energy to throw it into the top position where its potential energy may be maximized, therefore the balancing control is not needed. Yoshida et al. [3] put forward an energy-based swing-up control for the RIP system. It has been shown in [4] that the energy-based swing-up controller for the swing-up stage is effective. However, when the pendulum enters into the vicinity of the upright equilibrium position, the stability of the pendulum cannot be successfully guaranteed if there is a large disturbance suddenly applied to the pendulum. This phenomenon leads to the necessity of the balancing control, and it indicates the importance of choosing an efficient balancing controller.

In recent years, many modern control methodologies have been applied to the design of effective balancing controllers for the RIP system, such as adaptive control with time-varying uncertainties, composite fuzzy proportional-derivative control based on the referenced errors of state feedback, and neural networks control [5]-[7]. However, due to its complex nonlinearity in the RIP dynamic system, these methods are theoretically complicated and difficult to be directly implemented for the balancing control.

Simultaneously, several other control techniques, drawn

from nonlinear control theory [8], [9], including Lyapunov's direct method [10]-[12], and sliding mode control [13]-[15] are also discussed by many researchers. There always exists a difficult process to design an appropriate Lyapunov function to perform the theoretical stability analysis in these methods. Over the past years, optimal control theories attract more researchers' attention. Linear-quadratic regulator (LQR) is a typical optimal control scheme for the operation of a dynamic system. Park et al. [16] and Sukontanakarn and Parnichkun [17] both considered a LQR controller for the balancing control stage of the RIP system. In order to design a LQR controller, engineers always need to engage in an iterative process in which they evaluate the optimal controllers verified through numerical tests and then attune the parameters to produce a controller more consistent with design goals. However, the proper selection of the weighting factors in the cost function demands a strenuous procedure for the LQR based controller design. Besides that, due to the complex nonlinearity of our RIP dynamics, LQR as an optimal control scheme for linear systems is not optimal for the RIP system. In recent years, feedback linearization becomes the research interest due to its novel conversion from a nonlinear system dynamics to a fully or partly linear one. With this approach, the available linear control techniques can be utilized for the dynamic control [8]. Feedback linearization can be classified into two kinds: input-state feedback linearization (ISFL) and input-output feedback linearization (IOFL). Several cases [18], [19] with simple system dynamics can be proven input-state linearizable. However, due to the complexity of our RIP system dynamics, the satisfaction of conditions for applying ISFL method are hard to be algebraically developed, which is given in Theorem 6.2 in [8]. For that reason, we resort to the implementation of an IOFL controller [20]-[22] to the balancing control stage of the RIP system in this paper. And for this reason, the significance of conducting a comparison study between the Input-Output Feedback Linearization (IOFL) and the LQR draws our attention.

Linear-quadratic regulator (LQR) [23] is typically optimal for the control of a linear system, but may not necessarily for a nonlinear system. Input-output feedback linearization (IOFL) technique is commonly used in the controller design for a nonlinear system dynamics with the approach of converting the nonlinear system into a series of decoupled linear subsystems. The RIP is modeled as a fourth order nonlinear dynamics, and typically its control scheme is divided into two stages, i.e., a swing-up control and a balancing control. For the balancing stage, larger stability zone is desirable. The comparison of the stability regions of LQR and IOFL controllers for the nonlinear dynamics of the RIP during the balancing stage is studied. Designed by linearizing the nonlinear RIP system about the equilibrium point, LQR control provides stability within a vicinity of the equilibrium point. However, large disturbances can throw the RIP system into unstable status, and a swing-up control has to be reapplied to drive the pendulum into the sensitive equilibrium zone. The IOFL controller is designed based on the equivalent partially linearized subsystems transformed from the nonlinear system via employing a state transformation and an input transformation. Only the portion associated with two specific states out of the four in the nonlinear dynamics of RIP system can be linearized. For the linearized portion, its stability is governed by the linear control scheme, and its control input being applied into the unlinearizable portion of the original dynamics forms a closed loop, and this closed loop produces the so-called internal dynamics. However, further analysis reveals that the internal dynamics may not be guaranteed to be bounded input - bounded output (BIBO) stable. Due to this limitation, the stability zone of IOFL may not necessarily larger than that of LQR. This issue is treated with these techniques: For the linearized portion, pole placement is employed to provide a globally asymptotical stability so that no swing-up control stage is needed, and it induces the feedback gains associated with the angle and angular velocity of the inverted pendulum, thus the stability is enhanced. For the unlinearizable portion, the genetic algorithm [24] by minimizing the cost function is utilized to generate the gains associated with the angle and angular velocity of the rotary arm, thus an augmented stability is guaranteed by the genetic algorithm based IOFL technique. This paper presents a novel approach of pole-placement genetic algorithm synthesized IOFL control for RIP system, and the same concept can be applied in various nonlinear systems' control design. Simulink simulations are given to justify the theoretical analysis.

The paper is organized as follows: Section 2 derives the system dynamics of the RIP system and introduces the mathematical tools and theorems for designing LQR and conventional IOFL controllers. LQR and IOFL controllers are developed and the internal dynamics of the RIP system is discussed in Section 3. And the same section also includes the pole-placement genetic algorithm synthesized IOFL for augmented stability of the RIP control. Section 4 presents the simulation results. And the last section concludes the paper.

II. Modeling of a Rotary Inverted Pendulum System

A. Physical model

A rotary inverted pendulum is a complex electro-mechanical system. Fig. 1(a) shows a brief sketch of the RIP system and its main components.

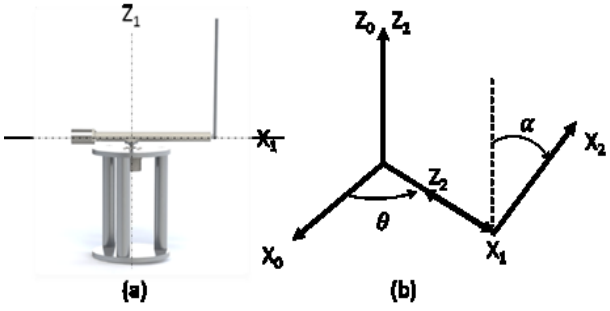

Fig. 1. (a) The physical model of the RIP system. (b) The coordinate system of the RIP system

The coordinate system of the RIP system is illustrated in Fig. 1(b). The fixed world coordinate frame is denoted with subscript 0. The frame $[X_1, Y_1, Z_1]$ is a body coordinate system of the rotary arm and $[X_2, Y_2, Z_2]$ is a body coordinate system of the pendulum arm. X_1 is aligned with the rotary arm and X_2 is aligned with the pendulum arm. The direction of Z_0 and Z_1 are both along the axis of the motor shaft. Let θ denote the angle between axes X_0 and X_1, and α be the angular displacement of the pendulum arm rotating clockwisely from the upright position. With the help of these coordinate systems, the system dynamics can be mathematically formulated using Lagrange's equation.

B. Mathematical Model

In order to apply Lagrange's equation, the velocity at the mass center of the rotary arm and the pendulum arm must be calculated at first. The coordinate of the mass center of the rotary arm is given as

$$\mathrm{P}_{02c} = R_z(\theta)T_x(l_1)R_y\left(-\frac{\pi}{2}\right)R_z(\alpha)P_{22c} \tag{1}$$

The coordinate at frame 2 is given as $[\mathrm{l}_{2c},\ 0,\ 0]^{\mathrm{T}}$. $\mathrm{R_z}$ and R_y are the rotational matrices about x axis and y axis, respectively. $\mathrm{T_x}$ is the translational matrix along x axis. The coordinate at frame 0 is given as

$$\mathrm{P}_{02c} = \begin{bmatrix} -l_{2c}\sin\theta\sin\alpha + l_1\cos\theta \\ l_{2c}\cos\theta\sin\alpha + l_1\sin\theta \\ l_{2c}\cos\alpha \end{bmatrix} \tag{2}$$

Let J denote the Jacobian matrix about vector P_{02c} with respect to $[\theta, \alpha]^{\mathrm{T}}$, the following equation is derived:

$$\begin{aligned} \dot{P}_{02c} &= J\begin{bmatrix}\dot{\theta}\\ \dot{\alpha}\end{bmatrix} \\ &= \begin{bmatrix} -l_{2c}\sin\alpha\cos\theta - l_1\sin\theta & -l_{2c}\sin\theta\cos\alpha \\ l_{2c}\sin\alpha\sin\theta + l_1\sin\theta & l_{2c}\cos\theta\cos\alpha \\ 0 & -l_{2c}\sin\alpha \end{bmatrix}\begin{bmatrix}\dot{\theta}\\ \dot{\alpha}\end{bmatrix} \end{aligned} \tag{3}$$

The angular velocity of the pendulum about its mass center in the frame 2 can also be determined as follows:

$$\begin{aligned} \omega_{22} &= \left(R_y\left(-\frac{\pi}{2}\right)R_z(\alpha)\right)^{-1}\begin{bmatrix}0\\0\\\dot{\theta}\end{bmatrix} + \begin{bmatrix}0\\0\\\dot{\alpha}\end{bmatrix} \\ &= \begin{bmatrix}\dot{\theta}\cos\alpha\\ -\dot{\theta}\sin\alpha\\ \dot{\alpha}\end{bmatrix} \end{aligned} \tag{4}$$

The RIP system consists of two rigid links, one is the horizontal rotary arm and another is the rotational pendulum arm. The energy as a summation of the kinetic energy and the potential energy for both arms are expressed as follows:

$$\begin{aligned} \mathrm{E}_1 &= E_{k1} + E_{p1} \\ \mathrm{E}_2 &= E_{k2} + E_{p2} \end{aligned} \tag{5}$$

Assume that $\mathrm{E}_{\mathrm{p1}} = 0$, since rotary arm is always parallel to the ground plane. $\mathrm{E}_{\mathrm{p2}} = 0$ is predefined when $\alpha = 0$, from which the formulas for $\mathrm{E}_{\mathrm{k1}}, E_{p1}, E_{k2}$ and E_{p2} can be derived:

$$\mathrm{E}_{\mathrm{k1}} = \frac{1}{2}(J_r + m_1 l_{1c}^2)\dot{\theta}^2 \tag{6}$$

$$\mathrm{E}_{\mathrm{k2}} = \frac{1}{2}m_2\left(\dot{P}_{02c}\right)^T\left(\dot{P}_{02c}\right) + \frac{1}{2}(\omega_{22})^T I_2\omega_{22} \tag{7}$$

$$\mathrm{E}_{\mathrm{p2}} = -m_2 g l_{2c}(1 - \cos\alpha) \tag{8}$$

Defining the Lagrangian $\mathrm{L} \overset{\text{def}}{=} \mathrm{E}_{\mathrm{k1}} + E_{k2} - E_{p1} - E_{p2}$, with two generalized coordinates θ and α, the following Lagrange's equation can be utilized to derive the system dynamics:

$$\frac{\mathrm{d}}{\mathrm{dt}}\frac{\partial L}{\partial\dot{\theta}} - \frac{\partial L}{\partial\theta} = -b_\theta\dot{\theta} + \tau_m + \tau_{C\theta} \tag{9}$$

$$\frac{\mathrm{d}}{\mathrm{dt}}\frac{\partial L}{\partial\dot{\alpha}} - \frac{\partial L}{\partial\alpha} = -b_\alpha\dot{\alpha} + \tau_{C\alpha} \tag{10}$$

Substituting (3) and (4) into (9) and (10), the system dynamics is obtained:

$$\begin{aligned} &(J_r + m_1 l_{1c}^2 + C_2\sin^2\alpha + I_{2xx}\cos^2\alpha \\ &\qquad + m_2 l_1^2)\ddot{\theta} \\ &\qquad + 2(C_2 \\ &\qquad - I_{2xx})\dot{\theta}\dot{\alpha}\sin\alpha\cos\alpha \\ &\qquad + C_3\ddot{\alpha}\cos\alpha - C_3\dot{\alpha}^2\sin\alpha \\ &\qquad = -b_\theta\dot{\theta} + \tau_m + \tau_{C\theta} \end{aligned} \tag{11}$$

$$\begin{aligned} \mathrm{C}_1\ddot{\alpha} + C_3\ddot{\theta}\cos\alpha - &(C_2 - I_{2xx})\dot{\theta}^2\sin\alpha\cos\alpha \\ &- C_4\sin\alpha = -b_\alpha\dot{\alpha} + \tau_{C\alpha} \end{aligned} \tag{12}$$

where in (11) and (12), the coefficients are summarized in Table 1.

Table 1: Summarized coefficients of the system dynamics

$\mathrm{C}_1 = I_{2zz} + m_2 l_{2c}^2$	$\mathrm{C}_2 = I_{2yy} + m_2 l_{2c}^2$
$\mathrm{C}_3 = m_2 l_1 l_{2c} - I_{2xz}$	$\mathrm{C}_4 = m_2 g l_{2c}$

Table 2: Parameters by system identification

$\mathrm{C}_1 = 9.667 \times 10^{-4}$	$\mathrm{C}_6 = 1.078 \times 10^{-6}$
$\mathrm{C}_2 = 9.731 \times 10^{-4}$	$\mathrm{b}_\alpha = 6.500 \times 10^{-6}$
$\mathrm{C}_3 = 9.404 \times 10^{-4}$	$\mathrm{b}_\theta = 2.973 \times 10^{-5}$
$\mathrm{C}_4 = 0.0689$	$\tau_{C\theta} \approx 0$
$\mathrm{C}_5 = 0.0017$	$\tau_{C\alpha} \approx 0$

The moment of inertia matrix of the pendulum is I_2 which has the form

$$\mathrm{I}_2 = \begin{bmatrix} \mathrm{I}_{2xx} & \mathrm{I}_{2xy} & \mathrm{I}_{2xz} \\ \mathrm{I}_{2yx} & \mathrm{I}_{2yy} & \mathrm{I}_{2yz} \\ \mathrm{I}_{2zx} & \mathrm{I}_{2zy} & \mathrm{I}_{2zz} \end{bmatrix}$$

By system identification, a group of valid parameters is provided for studying the system dynamics (see Table 2).

C. LQR and Input-Output Feedback Linearization

For a Linear time invariant (LTI) system

$$\begin{aligned} \dot{x} &= Ax + Bu \\ \mathrm{y} &= \mathrm{Cx} \end{aligned} \tag{13}$$

Infinite-horizon, continuous-time LQR scheme is defined with a cost function

$$\mathrm{CF} = \int_0^\infty (x^T Q x + u^T R u + 2x^T N u)dt \qquad (14)$$

The feedback control law to minimize the cost function can be given as

$$\mathrm{u} = -\mathrm{K}x \qquad (15)$$

where $\mathrm{K} = \mathrm{R}^{-1}(B^T P + N^T)$, and P is determined by algebraic Riccati equation

$$\mathrm{A}^{\mathrm{T}}P + PA - (PB + N)R^{-1}(B^T P + N^T) + Q = 0 \qquad (16)$$

For a nonlinear system represented as an affine form

$$\dot{x} = f(x) + g(x)u$$
$$\mathrm{y} = \mathrm{h}(\mathrm{x}) \qquad (17)$$

The input-output feedback linearization is iterated step by step.

$$\dot{y} = \nabla h(f + gu) \stackrel{\text{def}}{\equiv} L_f h(x) + L_g h(x) u \qquad (18)$$

If $\mathrm{L_g}h(x) \neq 0$ for all x in the operational region, the input transformation can be given as

$$\mathrm{u} = \frac{1}{\mathrm{L_g h}}\left(-L_f h + v\right) \qquad (19)$$

Equation (19) will result in a linear relation between input and output as

$$\dot{y} = v \qquad (20)$$

If $\mathrm{L_g}h(x) = 0$ for all x in the operational region, differentiating y again and so on until the r-th derivative of y results in $\mathrm{L_g}L_f^{r-1}h(x) \neq 0$, then the control law is derived as

$$\mathrm{u} = \frac{1}{\mathrm{L_g L_f^{r-1} h}}\left(-L_f^r h + v\right) \qquad (21)$$

Control law (21) yields a linear relationship between input and output as

$$\mathrm{y}^{(\mathrm{r})} = v \qquad (22)$$

The number of differentiation r is called the relative degree of the system. It is verified in the next section that the relative degree of the RIP system is 2. With the linear relationship between input and output shown in (22), the controller based on linear control theory, for instance, the pole placement techniques, can be designed.

III. Controller Design and the Internal Dynamics Analysis

A. *LQR Controller Design*

In order to design the LQR controller, the nonlinear dynamics (11) and (12) is linearized into a linear form. The nonlinear Coulomb friction terms are automatically dropped, and the last terms are linearized about the equilibrium point $[\theta \quad \dot{\theta} \quad \alpha \quad \dot{\alpha}]^T = [0 \quad 0 \quad 0 \quad 0]^T$. The state space model (13) can be obtained with

$$\mathrm{A} = \begin{bmatrix} 0 & 1 & 0 & 0 \\ 0 & -\frac{C_1 b_\theta}{C_1 C_5 - C_3^2} & -\frac{C_3 C_4}{C_1 C_5 - C_3^2} & \frac{C_3 b_\alpha}{C_1 C_5 - C_3^2} \\ 0 & 0 & 0 & 1 \\ 0 & \frac{C_3 b_\theta}{C_1 C_5 - C_3^2} & \frac{C_4 C_5}{C_1 C_5 - C_3^2} & -\frac{C_5 b_\alpha}{C_1 C_5 - C_3^2} \end{bmatrix} \qquad (23)$$

$$\mathrm{B} = \begin{bmatrix} 0 \\ \frac{C_1}{C_1 C_5 - C_3^2} \\ 0 \\ -\frac{C_3}{C_1 C_5 - C_3^2} \end{bmatrix} \qquad C = \begin{bmatrix} 0 \\ 0 \\ 1 \\ 0 \end{bmatrix} \qquad (24)$$

where $\mathrm{C}_1, C_2, C_3, C_4$ are given in Section 2.2 and $\mathrm{C}_5 = J_r + m_1 l_{1c}^2 + I_{2xx} + m_2 l_1^2$. Iteratively setting proper values to Q, R and N by verifying the performance of the LQR controller, the simulation can be performed, and the simulated results using the LQR controller are presented in Section 4 to compare with the results of IOFL.

B. *IOFL Controller Design*

The system dynamics (11) and (12) is represented into the affine form (17).

$$\begin{bmatrix} \dot{\theta} \\ \ddot{\theta} \\ \dot{\alpha} \\ \ddot{\alpha} \end{bmatrix} = \begin{bmatrix} \dot{\theta} \\ \frac{1}{\det(M)}(C_1 \tau_m + a - b) \\ \dot{\alpha} \\ \frac{1}{\det(M)}(-C_3 \cos\alpha\, \tau_m + c - d) \end{bmatrix} \qquad (25)$$

where M, C_6, a, b, c, d are simplified coefficients which are directly derived from coefficients given in Table 2. These new coefficients which are used to reduce the complexity of matrix inversion operations in the calculation are given as follows:

$$\mathrm{M} = \begin{bmatrix} C_2 \sin^2\alpha + C_5 + I_{2xx}\cos^2\alpha & C_3 \cos\alpha \\ C_3 \cos\alpha & C_1 \end{bmatrix} \qquad (26)$$

$$\mathrm{C}_6 = C_2 - I_{2xx}$$

$$\mathrm{a} = \mathrm{C}_1\left((-b_\theta - C_6 \sin 2\alpha\, \dot{\alpha})\dot{\theta} + C_3 \sin\alpha\, \dot{\alpha}^2 + \tau_{C\theta}\right) \qquad (27)$$

$$\mathrm{b} = \mathrm{C}_3 \cos\alpha\left(\frac{C_6}{2}\sin 2\alpha\, \dot{\theta}^2 - b_\alpha \dot{\alpha} + C_4 \sin\alpha + \tau_{C\alpha}\right) \qquad (28)$$

$$\mathrm{c} = (C_5 + I_{2xx}\cos^2\alpha + C_2 \sin^2\alpha) \cdot \left(C_4 \sin\alpha + \frac{C_6}{2}\sin 2\alpha\, \dot{\theta}^2 - b_\alpha \dot{\alpha} + \tau_{C\alpha}\right) \qquad (29)$$

$$\mathrm{d} = \mathrm{C}_3 \cos\alpha\left((-b_\theta - C_6 \sin 2\alpha\, \dot{\alpha})\dot{\theta} + C_3 \sin\alpha\, \dot{\alpha}^2 + \tau_{C\theta}\right) \qquad (30)$$

By observing (25) and applying control law (21), we found control law should be as

$$u = \tau_m = \frac{\det(M)\, v - c + d}{-C_3 \cos\alpha} \quad (31)$$

This control law will render the linear relationship between the input and output such as

$$\ddot{y} = v = -K_3 \cdot \alpha - K_4 \cdot \dot{\alpha} \quad (32)$$

C. *Internal Dynamics Analysis*

The internal dynamics of the RIP system is given as

$$\ddot{\theta} = \frac{1}{\det(M)}(C_1 u + a - b) \quad (33)$$

Pluging (31) into (33), the complete form of the internal dynamics can be obtained. With the aim of analyzing the steady state behavior of the internal dynamics, the concept of zero dynamics can be introduced, i.e., the dynamics of the system (17) should satisfy the conditions that the output should be identically zero. The zero dynamics associated with θ is given as

$$\ddot{\theta} = 0 \quad (34)$$

The equation (34) is obtained, by forcing $v, \alpha, \dot{\alpha}$ equal to identically 0. It shows from (34) that the internal dynamics will have a form as

$$\theta = pt + q \quad (35)$$

where p and q are both constant real values. This will yield a behavior that the α response is asymptotically stable while θ response is unbounded as a result. With the intention of stabilizing the un-linearized portion of the RIP dynamics, i.e., the dynamics associated with θ and $\dot{\theta}$, a full state feedback should be considered.

D. Pole-Placement Genetic Algorithm Synthesized IOFL Controller

The control law associated with (19) and (20) is pre-formulated as

$$v = -K_1 \cdot \theta - K_2 \cdot \dot{\theta} - K_3 \cdot \alpha - K_4 \cdot \dot{\alpha} \quad (36)$$

The values of K_1, K_2, K_3 and K_4 need to be determined. The linearized portion of the RIP dynamics is described as

$$\frac{d}{dt}\tilde{x} = \frac{d}{dt}\begin{bmatrix}\alpha \\ \dot{\alpha}\end{bmatrix} = \begin{bmatrix}\dot{\alpha} \\ v\end{bmatrix} = \begin{bmatrix}0 & 1 \\ 0 & 0\end{bmatrix}\tilde{x} + \begin{bmatrix}0 \\ 1\end{bmatrix} v \quad (37)$$

The pole placement for stabilizing the system dynamics (37) is utilized to determine K_3 and K_4. However, in order to reduce the influence of the undecided K_1, K_2 and un-linearized θ dynamics on the stability of the linearized α dynamics, the poles of the closed form of (37) are placed far left from the imaginary axis.

In the case of RIP system, the poles are chosen as $[-40, -20]$, with which the gains can be determined as $K_3 = 800$ and $K_4 = 60$. It is found that these gains K_3 and K_4 can ensure that the addition of $-K_1 \cdot \theta - K_2 \cdot \dot{\theta}$ to the control input v will not affect the stability of linearized portion of the RIP dynamics $\alpha, \dot{\alpha}$ when K_1 and K_2 are selected in the specific ranges, such that $K_1 \in [-20, 0]$ and $K_2 \in [-20, -10]$, and it will not severely degrade the stability of $\alpha, \dot{\alpha}$ dynamics.

Genetic algorithm (GA) is employed to get the optimal K_1 and K_2 gains in the prescribed intervals for K_1 and K_2 (feasible sets). The cost function to be minimized is specified as

$$f(K) = \left(1 - e^{-\beta}\right)\left(M_p + E_{ss}\right) + e^{-\beta}(t_s - t_r) \quad (38)$$

where M_p, E_{ss}, t_s and t_r are the overshoot, steady state error, settling time and rising time of the α response. β is the weighted factor affecting the proportion of the sum of overshoot and steady state error to the difference of settling time and rising time. In the simulation $\beta = 0.5$ is empirically chosen to minimize the effect of $t_s - t_r$. Then, the global optimization problem can be formulated as

$$K_1, K_2 = \underset{\substack{K_1 \in [-20,0] \\ K_2 \in [-20,-10]}}{\arg\min} f(K) \quad (39)$$

The genetic algorithm is applied to the optimization problem (39) with parameters listed in Table 3.

Table 3. Parameters selected for genetic algorithm

Population size = 10	Crossover rate = 0.5
Mutation rate = 0.01	Generation number = 25

As a result of GA based IOFL design techniques synthesis, the optimal full state feedback controller design is attained for the RIP system, and the gains are determined as

$$K_1 = -9.014 \quad K_2 = -15.276 \quad K_3 = -800 \quad K_4 = -60$$

IV. Simulation Results

The simulation block with IOFL controller is shown in Fig. 2. In this model, the mechanical dynamics of the RIP system and its control is presented. The modeling of its sensors and actuators demonstrates much higher frequency bands than the mechanical dynamics of the RIP system. Without loss of generality, simplifying the modeling of the sensors and actuators will not invalidate the controller design and its stability analysis of the whole system, since a compensator can be added to counterbalance the effects of the sensors and actuators in the real system. The Simulink block with LQR controller is similar to Fig. 2, the only difference is that the input (15) is directly applied to the nonlinear dynamics (11) and (12).

The system simulation results for LQR controller are shown in Fig. 3 and Fig. 4. As it shows, LQR can only stabilize the pendulum arm when the perturbation is less than 0.6 rad away from its equilibrium point: In Fig. 3, the pendulum arm can return to the upright position when the initial state is $\alpha_0 = 0.1$ rad. However, the pendulum arm will rotate a whole round (2π rad) to get back to the equilibrium point when the initial state is $\alpha_0 = 0.6$ rad as shown in Fig. 4. It is found that even when the initial state a little bit larger than 0.6 rad, the pendulum arm loses its stability.

The system simulation for the pole-placement GA synthesized IOFL controller is shown in Fig. 5 and Fig. 6. From Fig. 6, it is found that the pole-placement GA synthesized IOFL controller can enlarge the stability region of the pendulum dynamics from roughly [0 rad, 0.6 rad] in LQR case to a much larger region [0 rad, π rad]. According to the symmetry of the pendulum arm rotating plane with

respect to the up-down direction, the pole-placement GA synthesized IOFL balancing controller is globally asymptotically stable when perturbations of the state α.

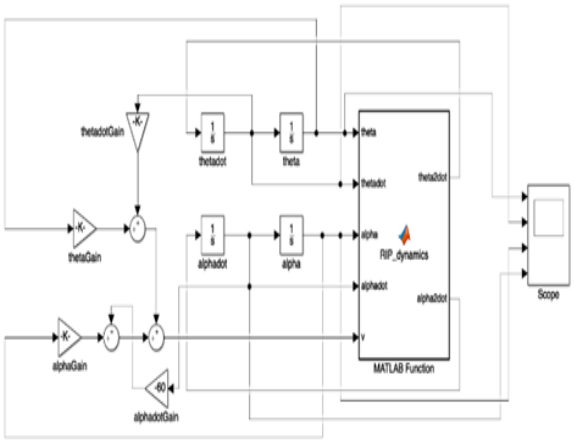

Fig. 2. The Simulink model of the RIP system with IOFL controller

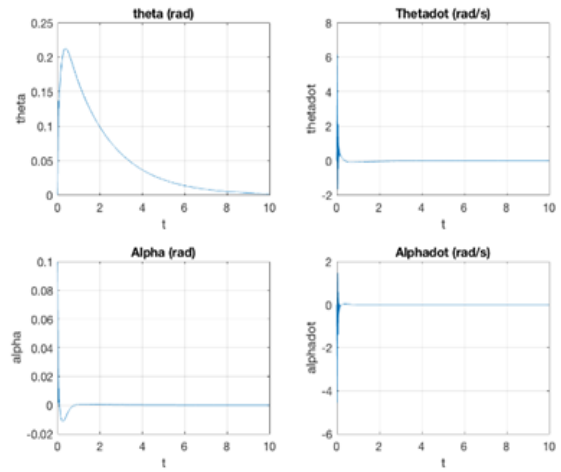

Fig. 3. System simulation with LQR controller, $\alpha_0 = 0.1\,rad$ (5.73 deg)

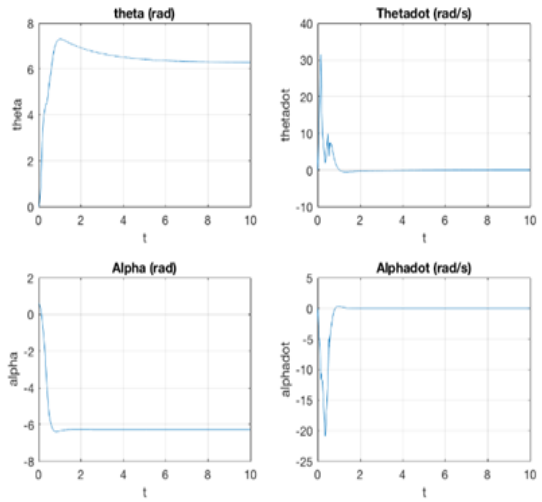

Fig. 4. System simulation with LQR controller, $\alpha_0 = 0.6\,rad$ (180 deg)

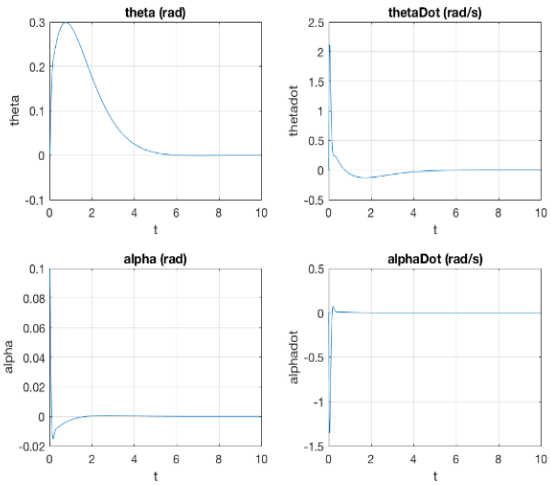

Fig. 5. System simulation with modified IOFL controller, $\alpha_0 = 0.1\,rad$ (5.73 deg)

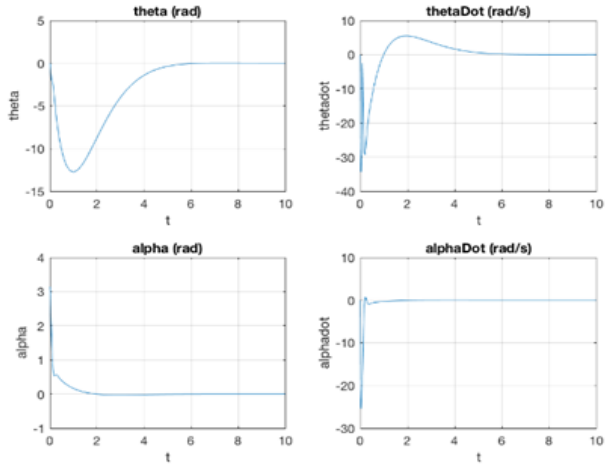

Fig. 6. System simulation with modified IOFL controller, $\alpha_0 = \pi\,rad$ (180 deg)

V. Conclusion

In this paper, per the analysis of internal dynamics of the RIP system, it is found that the conventional IOFL controller may not stabilize the rotary arm and the pendulum arm simultaneously, thus the balancing performance of the conventional IOFL controller may not be better than that of the LQR controller.

As a solution, a pole-placement genetic algorithm synthesized IOFL controller is presented. It is revealed that the modified IOFL controller can not only enlarge the stability region by bringing the pendulum arm to the upright equilibrium point without using an extra swing-up controller, but also effectively ensure the stability of the internal dynamics of the RIP system.

It is noticed that the modified IOFL controller has a limitation: the dynamic response of the rotary arm (the internal dynamics) has a large overshoot before it returns back to zero position. However, this issue will not severely degrade the overall performance of the modified IOFL controller in the balancing control of the RIP system.

This novel and synthesized control technique developed in this paper is valid for the nonlinear RIP system control. Without loss of its generality, the identical technique can be extensively applied in the controller design for various other complex dynamic systems.

APPENDIX

Nomenclature

θ Angular displacement of the rotary arm (rad)
α Angular displacement of the pendulum arm (rad)
$\dot{\theta}$ Angular velocity of the rotary arm (rad/s)
$\dot{\alpha}$ Angular velocity of the pendulum arm (rad/s)
l_1 Length of the rotary arm (m)
l_2 Length of the pendulum arm (m)
l_{1c} Distance of rotary arm's mass center to the axis of rotation (m)
l_{2c} Distance of pendulum arm's mass center to the two arms' linking point (m)
m_1 Mass of the rotary arm (kg)
m_2 Mass of the pendulum arm (kg)
J_r Rotational inertia of the rotary arm (kg· m^2)
I_2 Moment of inertia matrix of the pendulum arm (kg· m^2)
E_{k1} Kinetic energy of the rotary arm (J)
E_{k2} Kinetic energy of the pendulum arm (J)
E_{p1} Potential energy of the rotary arm (J)
E_{p2} Potential energy of the pendulum arm (J)
b_θ Damping ratio of the rotary arm about its rotational point (N· m · s/rad)
b_α Damping ratio of the pendulum arm about its link with the rotary arm (N· m · s/rad)
τ_m DC motor torque or control input (N· m)
$\tau_{C\theta}$ Coulomb friction of the rotary arm about its rotational point (N· m)
$\tau_{C\alpha}$ Coulomb friction of the pendulum arm about its link with the rotary arm (N· m)

REFERENCES

[1] Furuta, K., Yamakita, M., & Kobayashi, S., "Swing up control of inverted Pendulum," in International Conference on Industrial Electronics, Control and Instrumentation, 1991.
[2] Hemami, H., & Golliday Jr., C.L., "The inverted pendulum and biped stability," Mathematical Biosciences, vol. 34, no. 1-2, pp. 95-110, 1977.
[3] K. Yoshida, "Swing-up control of an inverted pendulum by energy-based methods," in Proceedings of the American Control Conference, San Diego, California, 1999.
[4] Åström, K. J., & Furuta, K., "Swing up a pendulum by energy control," Automatica, vol. 36, no. 2, pp. 287-295, 2000.
[5] Chen, Y., & Huang, A., "Adaptive control of rotary inverted pendulum system with time-varying uncertainties," Nonlinear Dynamics, pp. 95-102, 2014.
[6] J. Li, "Composite fuzzy control of a rotary inverted pendulum," in IEEE International Symposium on Industrial Electronics, 2013.
[7] Quyen, N. D., Thuyen, N. V., Hoc, N. Q., & Hien, N. D., "Rotary inverted pendulum and Control of Rotary inverted pendulum by artificial neural network," in Proceedings of National Theoretical Physics Conference, 2012.
[8] Slotine, J.-J. E., & Li, W., Applied Nonlinear Control, Englewood Cliffs, N.J.: Prentice Hall, 1991.
[9] H. K. Khalil, Nonlinear systems, Upper Saddle River, N.J.: Prentice Hall, 2002.
[10] Aguilar-Ibáñez, C., Suarez-Castañón, M. S., & Gutiérres-Frias, O. O., "The direct Lyapunov method for the stabilisation of the Furuta pendulum," International Journal of Control, vol. 83, no. 11, pp. 2285-2293, 2010.
[11] Türker, T., Görgün, H., & Cansever, G., "Lyapunov's direct method for stabilization of the Furuta pendulum," Turkish Journal of Electrical Engineering & Computer Sciences, vol. 20, no. 1, pp. 99-110, 2012.
[12] Wen, J., Shi Y., & Lu X., "Stabilizing a rotary inverted pendulum based on Lyapunov stability theorem," in 29th Chinese Control and Decision Conference (CCDC), Chongqing, China, 2017.
[13] Khanesar, M. A., Teshnehlab, M., & Shoorehdeli, M. A., "Sliding mode control of Rotary Inverted Pendulum," in Mediterranean Conference on Control & Automation, Athens, Greece, 2007.
[14] Zhang, Y., Ang, W.T., Jin, J., Zhang, S., & Man, Z., "Nonlinear Adaptive Sliding Mode Control for a Rotary Inverted Pendulum," Advances in Industrial Engineering and Operations Research, vol. 5, pp. 345-360, 2008.
[15] Faradja, P., Qi, G., & Tatchum, M., "Sliding mode control of a Rotary Inverted Pendulum using higher order differential observer," in 14th International Conference on Control, Automation and Systems, 2014.
[16] Park, M., Kim, Y., & Lee, J., "Swing-up and LQR stabilization of a rotary inverted pendulum," Artificial Life and Robotics, vol. 16, no. 1, pp. 94-97, 2011.
[17] Sukontanakarn, V., & Parnichkun, M., "Real-Time Optimal Control for Rotary Inverted Pendulum," American Journal of Applied Sciences, vol. 6, no. 6, pp. 1106-1115, 2009.
[18] Chen C., Lin C., & Yao, L., "Input-state linearization of a rotary inverted pendulum," Asian Journal of Control, vol. 6, no. 1, pp. 130-135, 2004.
[19] Ninomiya, T., Yamaguchi, I., & Kida, T., "Feedback Control of Plants Driven by Nonlinear Actuators via Input-State Linearization," Journal of Guidance, Control, and Dynamics, vol. 29, no. 1, pp. 20-24, 2006.
[20] Hauser, J., Sastry, S., & Kokotovic, P., "Nonlinear control via approximate input-output linearization: the ball and beam example," IEEE Transactions on Automatic Control, vol. 37, no. 3, pp. 392-398, 1992.
[21] Hassanzadeh, I., & Mobayen, S., "GA based input-output feedback linearization controller for rotary inverted pendulum system," in 5th International Symposium on Mechatronics and Its Applications, Amman, Jordan, 2008.
[22] Huang, A., & Yu, S., "Input-output feedback linearization control of uncertain systems using function approximation techniques," in 12th World Congress on Intelligent Control and Automation (WCICA), Guilin, China, 2016.
[23] Kwakernaak, H., & Sivan, R., Linear optimal control systems, New York: Wiley Interscience, 1972.
[24] Chong, E. K. P., & Zak, S. H., An Introduction to Optimization, 4 ed., vol. 76, John Wiley & Sons, 2013.

AUTHORS' PROFILES

Yi Yang
Is currently a Ph.D. student in School of Engineering Technology at Purdue University. He has received BS degree in Mechanical Engineering from Huazhong University of Science and Technology in 2015, and MS degree from The University of Michigan at Ann Arbor in 2017. Yi's research interest lies in the nonlinear system control, and mechatronics design. He is also interested in developing computer programs to solve optimization problems in industry or academia.

Haiyan Henry Zhang - is an Associate Professor of Engineering Technology and the founding director of Center for Technology Development at Purdue University. He received his Ph.D. from University of Michigan-Ann Arbor in 1996. With the multidisciplinary engineering background and industrial experience, his research foci are analytical mechatronic design, advanced manufacturing control, and design of traditional or hybrid electric vehicle powertrains.